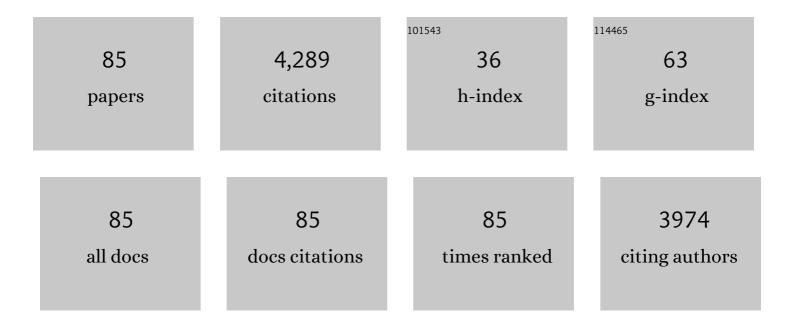
List of Publications by Year in descending order

Source: https://exaly.com/author-pdf/3593116/publications.pdf Version: 2024-02-01



ΖΗΙCΗΤΙΝ SI

#	Article	IF	CITATIONS
1	A Facile One Step Synthesis of MoS2/g-C3N4 Photocatalyst with Enhanced Visible Light Photocatalytic Hydrogen Production. Catalysis Letters, 2022, 152, 972-979.	2.6	8
2	Improved hydrothermal durability of Cu-SSZ-13 NH3-SCR catalyst by surface Al modification: Affinity and passivation. Journal of Catalysis, 2022, 405, 199-211.	6.2	28
3	A strategy to construct a highly active Co <sub><i>x</i></sub> P/SrTiO <sub>3</sub> (Al) catalyst to boost the photocatalytic overall water splitting reactions. Nanoscale, 2022, 14, 2427-2433.	5.6	5
4	An isolation strategy to anchor atomic Ni or Co cocatalysts on TiO2(A) for photocatalytic hydrogen production. Nano Research, 2022, 15, 5848-5856.	10.4	20
5	Combining Cu-SSZ-13 with TiO <sub>2</sub> : promotion of urea decomposition and influence on SCR. Reaction Chemistry and Engineering, 2022, 7, 2121-2131.	3.7	2
6	Tungsten Oxide Modified V2O5-Sb2O3/TiO2 Monolithic Catalyst: NH3-SCR Activity and Sulfur Resistance. Processes, 2022, 10, 1333.	2.8	0
7	Quasi- <i>operando</i> quantification of Cu( <scp>ii</scp> ) ions in Cu-SSZ-13 catalyst by an NH <sub>3</sub> temperature-programmed reduction method. Chemical Communications, 2021, 57, 1891-1894.	4.1	13
8	Nitrogen doped graphene quantum dots as a cocatalyst of SrTiO <sub>3</sub> (Al)/CoO <sub>x</sub> for photocatalytic overall water splitting. Catalysis Science and Technology, 2021, 11, 3039-3046.	4.1	17
9	Stable Pt atomic clusters on carbon nanotubes grafted with carbon quantum dots as electrocatalyst for H <sub>2</sub> evolution in acidic electrolyte. Nano Select, 2021, 2, 2126-2134.	3.7	7
10	Graphene quantum dots piecing together into graphene on nano Au for overall water splitting. Carbon, 2021, 178, 265-272.	10.3	17
11	Ni single atoms anchored on nitrogen-doped graphene as H2-Evolution cocatalyst of SrTiO3(Al)/CoO for photocatalytic overall water splitting. Carbon, 2021, 183, 763-773.	10.3	22
12	High-surface-area SmMn2O5 nanosheets with crystal orientation for propane combustion: A facile microwave-assisted hydrothermal method. Fuel, 2021, 306, 121685.	6.4	11
13	Potassium deactivation of Cu-SSZ-13 catalyst for NH3-SCR: Evolution of salts, zeolite and copper species. Chemical Engineering Journal, 2020, 383, 123080.	12.7	40
14	Facile method of synthesizing multilayer graphene capsuled sulfur nanoparticles for water treatment. Applied Surface Science, 2020, 502, 144194.	6.1	9
15	Critical roles of Cu(OH)2 in low-temperature moisture-induced degradation of Cu-SAPO-34 SCR catalyst: Correlating reversible and irreversible deactivation. Applied Catalysis B: Environmental, 2020, 278, 119306.	20.2	35
16	MOF-derived (MoS <sub>2</sub> , γ-Fe <sub>2</sub> O <sub>3</sub> )/graphene Z-scheme photocatalysts with excellent activity for oxygen evolution under visible light irradiation. RSC Advances, 2020, 10, 17154-17162.	3.6	17
17	Comparative study of La1–Ce MnO3+ perovskites and Mn–Ce mixed oxides for NO catalytic oxidation. Journal of Rare Earths, 2020, 38, 863-872.	4.8	10
18	Pt@g-C3N4/CeO2 photocatalyst for the remediation of low concentration NO at room temperature. Progress in Natural Science: Materials International, 2020, 30, 308-311.	4.4	6

**Z**нісним Si

#	Article	IF	CITATIONS
19	Deposition of Potassium Salts on Soot Oxidation Activity of Cu-SSZ-13 as a SCRF Catalyst: Laboratory Study. Catalysis Surveys From Asia, 2020, 24, 250-258.	2.6	5
20	SmMn2O5 catalysts modified with silver for soot oxidation: Dispersion of silver and distortion of mullite. Applied Catalysis B: Environmental, 2020, 273, 119058.	20.2	56
21	Size effect of Pt nanoparticles in acid-assisted soot oxidation in the presence of NO. Journal of Environmental Sciences, 2020, 94, 64-71.	6.1	14
22	Relationships between copper speciation and BrÃ,nsted acidity evolution over Cu-SSZ-13 during hydrothermal aging. Applied Catalysis A: General, 2020, 602, 117650.	4.3	38
23	Low-Temperature Solid-State Ion-Exchange Method for Preparing Cu-SSZ-13 Selective Catalytic Reduction Catalyst. ACS Catalysis, 2019, 9, 6962-6973.	11.2	37
24	Synthesizing multilayer graphene from amorphous activated carbon via ammonia-assisted hydrothermal method. Carbon, 2019, 152, 24-32.	10.3	33
25	A comprehensive study on sulfur tolerance of niobia modified CeO2/WO3-TiO2 catalyst for low-temperature NH3-SCR. Applied Catalysis A: General, 2019, 580, 121-130.	4.3	40
26	Direct ink writing of porous cordierite honeycomb ceramic. Ceramics International, 2019, 45, 15230-15236.	4.8	21
27	Deactivation of Cu-SAPO-34 by urea-related deposits at low temperatures and the regeneration. Journal of Environmental Sciences, 2019, 81, 43-51.	6.1	7
28	Atomic palladium on graphitic carbon nitride as a hydrogen evolution catalyst under visible light irradiation. Communications Chemistry, 2019, 2, .	4.5	57
29	Facile synthesis of NaOH-promoted Pt/TiO2 catalysts for toluene oxidation under visible light irradiation. Applied Surface Science, 2019, 469, 246-252.	6.1	28
30	Pd–Ag@CeO <sub>2</sub> Catalyst of Core–Shell Structure for Low Temperature Oxidation of Toluene Under Visible Light Irradiation. Journal of Physical Chemistry C, 2019, 123, 1761-1769.	3.1	30
31	Quantitative control and identification of copper species in Cu–SAPO-34: a combined UV–vis spectroscopic and H2-TPR analysis. Research on Chemical Intermediates, 2019, 45, 1309-1325.	2.7	21
32	In situ synthesized MoS2/Ag dots/Ag3PO4 Z-scheme photocatalysts with ultrahigh activity for oxygen evolution under visible light irradiation. Applied Surface Science, 2018, 450, 441-450.	6.1	30
33	CoMoS2/rGO/C3N4 ternary heterojunctions catalysts with high photocatalytic activity and stability for hydrogen evolution under visible light irradiation. Applied Surface Science, 2018, 435, 1296-1306.	6.1	37
34	Noble metal-free NiS/P-S codoped g-C3N4 photocatalysts with strong visible light absorbance and enhanced H2 evolution activity. Catalysis Communications, 2018, 106, 55-59.	3.3	30
35	Synergistic effect of CeO 2 modified TiO 2 photocatalyst on the enhancement of visible light photocatalytic performance. Journal of Alloys and Compounds, 2017, 714, 560-566.	5.5	88
36	Decomposition behavior of ammonium nitrate on ceria catalysts and its role in the NH <sub>3</sub> -SCR reaction. Catalysis Science and Technology, 2017, 7, 2531-2541.	4.1	19

#	Article	IF	CITATIONS
37	Nb-modified Mn/Ce/Ti catalyst for the selective catalytic reduction of NO with NH 3 at low temperature. Applied Catalysis A: General, 2017, 545, 64-71.	4.3	99
38	Migration, reactivity, and sulfur tolerance of copper species in SAPO-34 zeolite toward NO <sub>x</sub> reduction with ammonia. RSC Advances, 2017, 7, 37787-37796.	3.6	13
39	Evolution of copper species on Cu/SAPO-34 SCR catalysts upon hydrothermal aging. Catalysis Today, 2017, 281, 596-604.	4.4	92
40	Localized Surface Plasmon Resonance Assisted Photothermal Catalysis of CO and Toluene Oxidation over Pd–CeO <sub>2</sub> Catalyst under Visible Light Irradiation. Journal of Physical Chemistry C, 2016, 120, 29116-29125.	3.1	62
41	A novel Au/r-GO/TNTs electrode for H2O2, O2 and nitrite detection. Sensors and Actuators B: Chemical, 2016, 234, 264-272.	7.8	23
42	Effect of lean-oxygen treatment on the adsorption and activity of zirconium phosphate @ Ce0.75Z0.25O2 for NH3-SCR deNO. Catalysis Today, 2016, 267, 47-55.	4.4	13
43	Effects of silica additive on the NH 3 -SCR activity and thermal stability of a V 2 O 5 /WO 3 -TiO 2 catalyst. Chinese Journal of Catalysis, 2016, 37, 1340-1346.	14.0	47
44	NH3-SCR reaction mechanisms of NbO /Ce0.75Zr0.25O2 catalyst: DRIFTS and kinetics studies. Journal of Molecular Catalysis A, 2016, 423, 172-180.	4.8	123
45	Optimizing the crystallinity and acidity of H-SAPO-34 by fluoride for synthesizing Cu/SAPO-34 NH3-SCR catalyst. Journal of Environmental Sciences, 2016, 41, 244-251.	6.1	22
46	Impacts of niobia loading on active sites and surface acidity in NbO /CeO2–ZrO2 NH3–SCR catalysts. Applied Catalysis B: Environmental, 2015, 179, 380-394.	20.2	210
47	Effects of WO3 doping on stability and N2O escape of MnO –CeO2 mixed oxides as a low-temperature SCR catalyst. Catalysis Communications, 2015, 69, 188-192.	3.3	43
48	The synthesis, activity, stability and the charge transfer identification of Ag:AgBr/γ-Al2O3 photocatalyst for organic pollutant decomposition in water. Applied Surface Science, 2015, 357, 1792-1800.	6.1	6
49	Low-temperature SCR activity and SO2 deactivation mechanism of Ce-modified V2O5–WO3/TiO2 catalyst. Progress in Natural Science: Materials International, 2015, 25, 342-352.	4.4	85
50	NH <sub>3</sub> -SCR activity, hydrothermal stability and poison resistance of a zirconium phosphate/Ce <sub>0.5</sub> Zr <sub>0.5</sub> O <sub>2</sub> catalyst in simulated diesel exhaust. RSC Advances, 2015, 5, 83594-83599.	3.6	18
51	Effect of water vapor on NH3–NO/NO2 SCR performance of fresh and aged MnOx–NbOx–CeO2 catalysts. Journal of Environmental Sciences, 2015, 31, 240-247.	6.1	32
52	Potassium poisoning on Cu-SAPO-34 catalyst for selective catalytic reduction of NOx with ammonia. Chemical Engineering Journal, 2015, 267, 191-200.	12.7	57
53	Selective catalytic reduction of NO by ammonia over phosphate-containing Ce0.75Zr0.25O2 solids. Applied Catalysis B: Environmental, 2015, 163, 223-232.	20.2	121
54	Durability of Cu/SAPO-34 catalyst for NO reduction by ammonia: Potassium and sulfur poisoning. Catalysis Communications, 2015, 59, 35-39.	3.3	33

#	Article	IF	CITATIONS
55	DRIFT Study of CuO–CeO <sub>2</sub> –TiO <sub>2</sub> Mixed Oxides for NO <sub><i>x</i></sub> Reduction with NH <sub>3</sub> at Low Temperatures. ACS Applied Materials & Interfaces, 2014, 6, 8134-8145.	8.0	247
56	Synthesis, characterization and photocatalytic activity of porous WO3/TiO2 hollow microspheres. Applied Surface Science, 2014, 313, 470-478.	6.1	48
57	Tailored temperature window of MnOx-CeO2 SCR catalyst by addition of acidic metal oxides. Chinese Journal of Catalysis, 2014, 35, 1281-1288.	14.0	21
58	Rare earth containing catalysts for selective catalytic reduction of NOx with ammonia: A Review. Journal of Rare Earths, 2014, 32, 907-917.	4.8	87
59	Facile synthesis of hierarchical porous γ-Al2O3 hollow microspheres for water treatment. Journal of Colloid and Interface Science, 2014, 417, 369-378.	9.4	35
60	Chemical deactivation of V2O5-WO3/TiO2 SCR catalyst by combined effect of potassium and chloride. Frontiers of Environmental Science and Engineering, 2013, 7, 420-427.	6.0	42
61	Tailored temperature window of CuOx/WOx–ZrO2 for NOx reduction via adjusting the calcination temperature of WOx–ZrO2. Materials Chemistry and Physics, 2013, 138, 399-404.	4.0	3
62	Lattice oxygen mobility and acidity improvements of NiO–CeO2–ZrO2 catalyst by sulfation for NOx reduction by ammonia. Catalysis Today, 2013, 201, 122-130.	4.4	83
63	Hydrothermal stability of MOx-Ce0.75Zr0.25O2 catalysts for NOx reduction by ammonia. Journal of Rare Earths, 2013, 31, 1148-1156.	4.8	19
64	Influences of impregnation procedure on the SCR activity and alkali resistance of V2O5–WO3/TiO2 catalyst. Applied Surface Science, 2013, 283, 209-214.	6.1	97
65	Highly dispersed iron species created on alkali-treated zeolite for ammonia SCR. Progress in Natural Science: Materials International, 2013, 23, 493-500.	4.4	22
66	Effects of WOx modification on the activity, adsorption and redox properties of CeO2 catalyst for NOx reduction with ammonia. Journal of Environmental Sciences, 2012, 24, 1305-1316.	6.1	97
67	Total oxidation of propane on Pt/WOx/Al2O3 catalysts by formation of metastable Ptî´+ species interacted with WOx clusters. Journal of Hazardous Materials, 2012, 225-226, 146-154.	12.4	102
68	Participation of sulfates in propane oxidation on Pt/SO42â^'/CeO2–ZrO2 catalyst. Journal of Molecular Catalysis A, 2012, 361-362, 98-103.	4.8	35
69	A novel Nb–Ce/WO –TiO2 catalyst with high NH3-SCR activity and stability. Catalysis Communications, 2012, 27, 97-100.	3.3	80
70	Synergistic effect between ceria and tungsten oxide on WO3–CeO2–TiO2 catalysts for NH3-SCR reaction. Progress in Natural Science: Materials International, 2012, 22, 265-272.	4.4	66
71	NH3-SCR activity, hydrothermal stability, sulfur resistance and regeneration of Ce0.75Zr0.25O2–PO43â~'catalyst. Catalysis Communications, 2012, 17, 146-149.	3.3	63
72	IR characterization of propane oxidation on Pt/CeO2–ZrO2: The reaction mechanism and the role of Pt. Journal of Molecular Catalysis A, 2012, 356, 100-105.	4.8	73

#	Article	IF	CITATIONS
73	Synergistic effects between copper and tungsten on the structural and acidic properties of CuOx/WOx–ZrO2 catalyst. Catalysis Science and Technology, 2011, 1, 453.	4.1	39
74	Effects of cerium and vanadium on the activity and selectivity of MnOx-TiO2 catalyst for low-temperature NH3-SCR. Journal of Rare Earths, 2011, 29, 64-68.	4.8	41
75	Modification of CeO2-ZrO2 catalyst by potassium for NOx-assisted soot oxidation. Journal of Environmental Sciences, 2011, 23, 145-150.	6.1	36
76	Structure, acidity and activity of CuOx/WOx–ZrO2 catalyst for selective catalytic reduction of NO by NH3. Journal of Catalysis, 2010, 271, 43-51.	6.2	137
77	NOx-assisted soot oxidation over K/CuCe catalyst. Journal of Rare Earths, 2010, 28, 542-546.	4.8	26
78	Roles of Lewis and BrÃ,nsted acid sites in NO reduction with ammonia on CeO2-ZrO2-NiO-SO42â^' catalyst. Journal of Rare Earths, 2010, 28, 727-731.	4.8	17
79	Modifications of CeO2–ZrO2 solid solutions by nickel and sulfate as catalysts for NO reduction with ammonia in excess O2. Catalysis Communications, 2010, 11, 1045-1048.	3.3	85
80	Photoinduced hydroxyl radical and photocatalytic activity of samarium-doped TiO2 nanocrystalline. Journal of Hazardous Materials, 2008, 150, 62-67.	12.4	322
81	Solar photocatalytic degradation of methylene blue in carbon-doped TiO2 nanoparticles suspension. Solar Energy, 2008, 82, 706-713.	6.1	196
82	Characterization and photocatalytic activity of Sm3+-doped TiO2 nanocrystalline prepared by low temperature combustion method. Journal of Alloys and Compounds, 2008, 450, 426-431.	5.5	50
83	Sol–gel auto-combustion synthesis of samarium-doped TiO2 nanoparticles and their photocatalytic activity under visible light irradiation. Materials Science and Engineering B: Solid-State Materials for Advanced Technology, 2007, 137, 189-194.	3.5	133
84	Effects of samarium dopant on photocatalytic activity of TiO2 nanocrystallite for methylene blue degradation. Journal of Materials Science, 2007, 42, 9194-9199.	3.7	28
85	Sub-Nano Pt/β-FeOOH Quantum Dots for Photocatalytic Removal of Toluene: Catalyst Design, Preparation, and Benefits. Frontiers in Materials, 0, 9, .	2.4	2